ARTICLE IN PRESS
JID: NMD [m5+;January 14, 2020;22:33]
Available online at www.sciencedirect.com
ScienceDirect
Neuromuscular Disorders xxx (xxxx) xxx
www.elsevier.com/locate/nmd

Cylindrical spirals in two families: Clinical and genetic investigations

Sarah J Beecroft[a], Montse Olive[b], Lidia Gonzalez Quereda[b], Maria Pia Gallano[b], Isabel Ojanguren[c], Catriona McLean[d], Pamela McCombe[e], Nigel G Laing[a], Gianina Ravenscroft[a,*]

[a] *Centre for Medical Research, University of Western Australia, Harry Perkins Institute of Medical Research, QEII Medical Centre, Australia*
[b] *Neuropathology Unit, Department of Pathology and Neuromuscular Unit, Department of Neurology, IDIBELL-Hospital de Bellvitge, Hospitalet de Llobregat, Barcelona 08907, Spain*
[c] *Department of Pathology, Hospital Germans Trias i Pujol, Badalona 08916, Spain*
[d] *Victorian Neuromuscular Laboratory, Alfred Health, Commercial Rd, Prahran, VIC 3181, Australia*
[e] *The University of Queensland Centre for Clinical Research, Royal Brisbane and Women's Hospital, Brisbane, Australia*

Received 22 October 2019; received in revised form 17 December 2019; accepted 19 December 2019
Available online xxx

Abstract

Cylindrical spirals are a rare ultrastructural finding on muscle biopsy, with fewer than 20 reported cases since its first description in 1979. These structures are sometimes observed with tubular aggregates and are thought to comprise longitudinal sarcoplasmic reticulum. While mutations in genes encoding key components of Ca^{2+} handling (*ORAI1* and *STIM1*) underlie tubular aggregate myopathy, no causative genes have been associated with cylindrical spirals. Here we describe two families with cylindrical spirals on muscle biopsy with a suspected genetic cause. In one family we identified a known truncating variant in *EBF3*, previously associated with a neurodevelopmental disorder. The affected individuals in this family present with clinical features overlapping with those described for *EBF3* disease. An isolated proband in the second family harbours bi-allelic truncating variants in *TTN* and her clinical course and other features on biopsy are highly concordant for titinopathy. From experimental studies, *EBF3* is known to be involved in Ca^{2+} regulation in muscle, thus EBF3 dysregulation may represent a novel mechanism of impaired Ca^{2+} handling leading to cylindrical spirals. Additional cases of *EBF3* disease or titinopathy with cylindrical spirals need to be identified to support the involvement of these genes in the pathogenesis of cylindrical spirals.

Keywords: Cylindrical spiral myopathy; EBF3; Next-generation sequencing; TTN; Tubular aggregates.

1. Introduction

Cylindrical spirals are an ultra-rare ultrastructural abnormality found in skeletal myofibres, with fewer than 20 published cases [1] since the first description in 1979 [2]. These whorled structures are characterised by accumulations of spiral lamellae, typically found under the sarcolemma in type II myofibres [1,2]. Cylindrical spirals are considered nonspecific due to the breadth of associated clinical features, ranging from muscle cramps exacerbated by exercise to severe congenital encephalomyopathy [2–11]. Although cylindrical spirals appear to be heritable in some cases [1], no genes have been associated with this feature. The pathomechanism leading to the formation of cylindrical spirals in skeletal muscle remains uncertain.

Cylindrical spirals have been seen to co-occur or be continuous with tubular aggregates, another rare ultrastructural abnormality comprised of membranous tubules in the sarcoplasm [12]. Tubular aggregates have been shown to arise from the whole sarcoplasmic reticulum (SR), therefore containing all components required for Ca^{2+} uptake, storage, and release [13]. In contrast, cylindrical spirals appear to arise from the longitudinal SR [1]. The genetic forms of tubular aggregate myopathy are caused by heterozygous mutations in *STIM1* and *ORAI1*, which produce constitutive activation of store operated Ca^{2+} entry [14]. The tubular aggregates may act a protective Ca^{2+} sink

* Corresponding author.
E-mail address: gina.ravenscroft@perkins.uwa.edu.au (G. Ravenscroft).

https://doi.org/10.1016/j.nmd.2019.12.006
0960-8966/

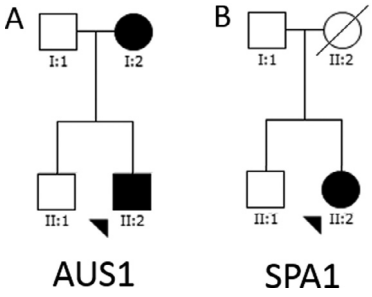

Fig. 1. Familial pedigrees. (A) Pedigree of Family AUS1, showing autosomal dominant transmission of the *EBF3* phenotype. (B) Pedigree of Family SPA1.

against the excessive cytosolic Ca^{2+} influx [12]. Given the co-occurrence and similar histological staining of tubular aggregates and cylindrical spirals [1,12], they may have a similar etiology (i.e. Ca^{2+} dysregulation). Previous studies showed that addition of Ca^{2+} to sonicated preparation of phosphatidylserine in aqueous NaCl buffer produces spiral shaped lipid cylinders that develop into flattened sheets, which then form coiled elongated multilamellar cylinders [5].

Here we describe two families (one from Australia, one from Spain) with cylindrical spirals as the hallmark feature on muscle biopsy. In the Australian family, a mother and son were both affected by an unclassified myopathy. In the Spanish family, the proband was diagnosed with congenital myopathy. Through familial exome sequencing, we reached a genetic diagnosis for both families, implicating *EBF3* and *TTN,* respectively. Thus, we have identified for the first time, as far as we are aware, genetic mutations that are associated with cylindrical spirals.

2. Patients and methods

This study was approved by the UWA Human Research Ethics Committee, and all patients gave informed consent.

2.1. Patient details

AUS1 was a non-consanguineous Caucasian quadruplex family from Australia (Fig. 1A). Mother and son were both affected, while both the older brother and father reported no symptoms. There were no other affected individuals in the mother's family. Muscle biopsies were taken from the mother at age 31, and her affected son at three years of age. DNA was available for all four family members.

SPA1 was a non-consanguineous family from Spain (Fig. 1B). The proband was a 39-year-old female. Her father and older brother were unaffected. Her mother had passed away many years prior due to hepatic failure. DNA was available for the proband, her father and her brother.

2.2. Genetic analysis

Whole exome sequencing (WES) was performed on both families, as previously described [15]. Genetic variants were annotated with Variant Effect Predictor [16] and stored a GEMINI [17] database for variant querying. Candidate pathogenic variants were confirmed with bi-directional Sanger sequencing [18] in all family members for whom we had DNA.

2.3. Muscle biopsy and histology

Muscle biopsies were taken as part of the clinical diagnostic investigation. The samples were immediately frozen in liquid nitrogen-cooled isopentane. 10 μm thick cryostat sections were stained with haematoxylin and eosin (H&E), modified Gomori trichrome, periodic acid Schiff (PAS), Oil red O, reduced nicotinamide adenine dinucleotide dehydrogenase-tetrazolium reductase (NADH-TR), succinic dehydrogenase (SDH), Cytochrome Oxidase (COX), and adenosine triphosphatase (ATPase) preincubated at pH 9.4, 4.63, 4.35. The Spanish sample underwent SERCA2 immunostaining. Small pieces of biopsied tissue were processed for ultrastructural examination using standard methods.

2.4. cDNA sequencing

In Family SPA1, a missense variant in *TTN* was identified, which was predicted to generate a cryptic splice site. To investigate the impact of this variant, we sequenced cDNA extracted from the proband's muscle biopsy. Primers were designed which included exon 54 to 55, and the region was PCR amplified. Primers and thermocycling conditions are available on request. The PCR product was run on a Qiaxel gel to visualise the product size in comparison to a healthy control sample. Following this, the PCR product was Sanger sequenced [18].

3. Results

3.1. Clinical findings

3.1.1. Family AUS1

As a child, AUS1 I:2 was grossly hypotonic with developmental delay and delayed motor milestones, walking at 2.5 years of age. She required ten years of speech therapy as a child. She had surgery for scoliosis at age 17 years. Examination in her mid-thirties revealed mild facial weakness with bilateral eyelid ptosis. She had a pointed chin, marked *pes planus*, very short thumbs bilaterally and a short great-toe on the right. She did not have scapular winging. Her muscle strength was globally reduced (MRC grade 4–5). She had trouble opening a jar and had a weak cough. She presented some problems with speech and co-ordination. She experienced cramps with strenuous exercise. There was no report of similarly affected siblings or parents. She appears to have improved with age.

AUS1 II:2 was markedly hypotonic in his trunk and neck at five weeks of age. At seven weeks he was diagnosed with laryngomalacia. Serum creatine kinase levels were

Please cite this article as: S.J. Beecroft, M. Olive and L.G. Quereda et al., Cylindrical spirals in two families: Clinical and genetic investigations, Neuromuscular Disorders, https://doi.org/10.1016/j.nmd.2019.12.006

480 U/L. Cranial ultrasound at three months of age was normal. He had poor, slow sucking during bottle feeding and periods of gagging or choking associated with cyanosis. He had delayed motor milestones, sitting at 13 months, cruising at 21 months, and walking at 27 months. He had poor/absent urinary excretion with a constant dribble stream since infancy. Bladder ultrasound at six months of age showed bladder diverticulae, particularly towards the bladder base. Additional ultrasound at age three years showed slight irregularity of the posterior wall of the bladder, suggestive of trabeculation. By age 7, daytime bladder function was normal, but night-time control was an issue. At age three, he showed global developmental delay, gait ataxia, flaccid muscle tone, but normal strength, sensation and reflexes. He experienced recurrent otitis media requiring removal of adenoids and placement of grommets. At age six he was described to have IQ in the low normal range. His cardiac assessment was normal. He would tire easily, and experience cramps, particularly after exercise. Features of Asperger's syndrome were noted and he was diagnosed with Pervasive Developmental Disorder at age 10. As a teenager, he was noted to have lower facial weakness and dysmorphic features (pointed chin). He had left scapular winging. He had surgery for scoliosis (age 13 years) and esotropia. Neuropsychological assessment at age 18 years showed a developmental delay in several areas, but he did not show intellectual impairment. He had poor ability at mathematics but performed well verbally.

3.1.2. Family SPA1

SPA1 II:2 was a 39-year-old female with congenital proximal and distal myopathy. She experienced mild delayed motor milestones, achieving head control at six months and walking at 18 months. She experienced frequent falls, was never able to run, and always had trouble with stairs. She developed progressive scoliosis requiring surgery at age 17. She subsequently developed restrictive ventilatory insufficiency requiring nocturnal ventilator support since age 22. She had proximal and distal muscle weakness that progressed very slowly over the years. Her creatine kinase level was normal. Examination at the age of 32 revealed bilateral Achilles contractures, distal joint hyperlaxity, bilateral *pes cavus* and scoliosis. There was global muscle hypotrophy and mild weakness involving all limbs. There was no facial weakness or ophthalmoplegia. Echocardiography and 24-hour Holter monitoring revealed episodes of non-sustained supraventricular tachycardia and mitral valve prolapse. Electromyography showed myogenic changes without spontaneous activity at rest, and no decremental response after repetitive nerve stimulation was observed.

3.2. Genetic results

3.2.1. Family AUS1

The affected mother and son were heterozygous for a known pathogenic truncating variant (c.616C>T, p.Arg206*) in *EBF3*, previously associated with an autosomal dominant neurodevelopmental syndrome [19]. This variant was absent in the unaffected father and brother. No likely pathogenic (class 4) or pathogenic (class 5) variants [20] were identified in other myopathy or neurologically related genes.

3.2.2. Family SPA1

The proband showed biallelic novel variants in *TTN* in exon 54 and 99 respectively; Chr2:179,598,095T>C; NM_001267550.1:c.15925A>G, p.Ile5309Val and Chr2:179,574,392G>A; NM_001267550.1: c.28654C>T, p.Gln9552*. The p.Gln9552* variant was paternally transmitted to both siblings, and absent from gnomAD [21]. Although maternal DNA was not available, the unaffected brother did not share the c.15925A>G, p.Ile5309Val variant, indicating the two variants are on different alleles. The p.Ile5309Val variant was strongly predicted to cause aberrant splicing by the multiple *in-silico* splicing prediction tools within the Alamut Software Suite (Interactive Biosoftware, Rouen, France; ESEfinder [22,23], Ex-Skip [24], GeneSplicer [25], Human Splicing Finder [26], MaxEntScan [27], NNSPLICE [25], RESCUE-ESE [28]). No likely pathogenic (class 4) or pathogenic (class 5) variants [20] were seen in other myopathy genes.

3.3. Pathology results

3.3.1. Family AUS1

Patient AUS1 I:2 was biopsied at age 31 years for diagnostic purposes. There was a modest type II myofibre atrophy (not shown). Around 80% of type II myofibres contained subsarcolemmal lesions which were sharply defined from the adjacent sarcoplasm, and basophilic on H&E staining (Fig. 3A). Some inclusions also showed some weak staining with NADH (Fig. 3B) and PAS. Electron microscopy showed cylindrical spirals. These were associated with free glycogen granules (Fig. 3C-D). Tubular aggregates were not seen.

Patient AUS1 II:2 was biopsied at age three. Approximately 10–15% of myofibres showed well-demarcated inclusions, which were often subsarcolemmal. By electron microscopy, aggregates of cylindrical spirals and scant associate tubular aggregate structures were present. Micrographs are not shown due to the poor resolution of the available images. Tissue is no longer available to perform further immunohistochemistry or imaging.

3.3.2. Family SPA1

At age 32 years, patient SPA1 II:2 underwent a biopsy which showed large numbers of internal nuclei (Fig. 3E). Approximately 10% of fibres showed subsarcolemal inclusions that were hardly seen on H&E (Fig. 3E), but appeared bright red on modified Gomori stain (Fig. 3F). They showed faint NADH activity (Fig. 3G). Moreover, there were some core-like lesions on oxidative stains (Fig. 3G). The inclusions did not immunostain with SERCA2 antibodies (not shown). Under electron microscopy the inclusions corresponded to spirals containing up to 12 concentric

Please cite this article as: S.J. Beecroft, M. Olive and L.G. Quereda et al., Cylindrical spirals in two families: Clinical and genetic investigations, Neuromuscular Disorders, https://doi.org/10.1016/j.nmd.2019.12.006

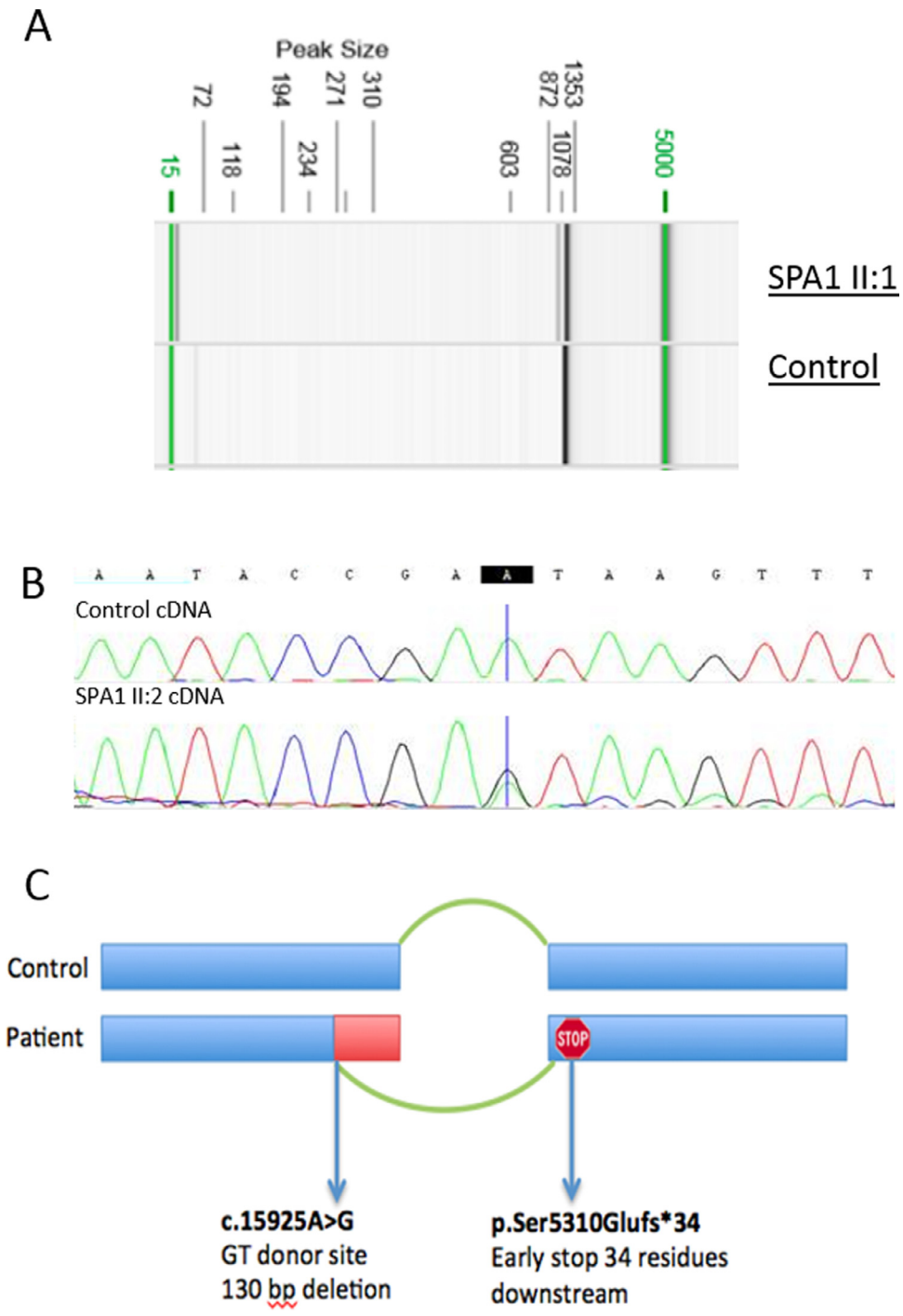

Fig. 2. Confirmation of *TTN* splice-site variant in family SPA1. (A) Qiaxel gel showing the difference in PCR amplicon size in *TTN* exons 54-55 in healthy control cDNA and patient SPA1 II:2. The patient showed a slightly smaller product in addition to the expected size, suggesting alternate splicing of one allele. (B) Sanger sequencing of the TTN exon 54-55 cDNA showed the c.15925A>G base change was present in SPA1 II:2, but not in the healthy control. (C) A schematic diagram of the predicted impact of the c.15925A>G base change on the *TTN* mRNA. The 130 base pair deletion causes an early stop codon downstream of the splice variant, likely resulting in nonsense mediated decay.

lamellae often seen under the sarcolemma and sometimes associated with tubular profiles (Fig. 3H-I). In addition, there were areas showing multiple foci of sarcomere disruption with fragmentation of Z-line and loss of thick myofilaments with dissolution of the M-line and A-line (Fig. 3J-L).

3.4. cDNA sequencing

The exon 54–55 *TTN* cDNA PCR product from patient SPA1 II:2 and a healthy control were run on a Qiaxel gel to visualise the size of the PCR product. SPA1 II:2

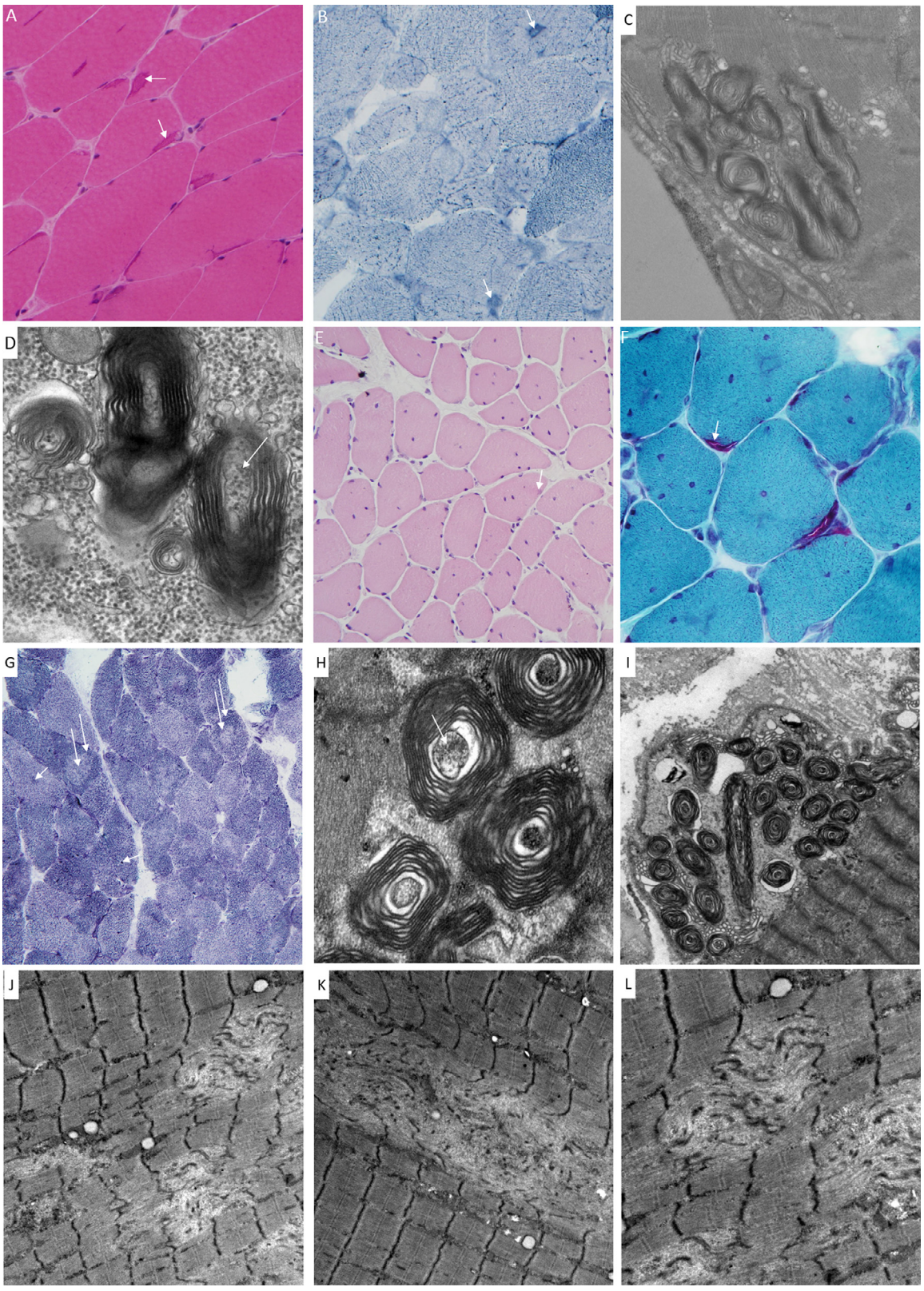

Fig. 3. Muscle histology from affected patients. (A-D) AUS1 I:2 and (E-L) SPA1 II:2. Muscle from patient AUS1 I:2 showed inclusions (arrows) strongly demarcated with H&E staining (A), that were also faintly positive for NADH (B). Electron microscopy of AUS1 I:2 showed subsarcolemmal accumulation of cylindrical spirals (C). Higher magnification shows glycogen granules around the cylindrical spirals and within the core (indicated with arrow) (D). Patient SPA1 II:2 showed large numbers of internal nuclei and faintly detectable inclusions on H&E (E). These inclusions were clearly detected with modified Gomori trichrome (F) and occurred sub-sarcolemmally. The inclusions displayed faint NADH activity (G). Moreover, there were some core-like lesions (double arrows in G). Electron microscopy showed cylindrical spiral structures (H and I) associated with glycogen granules in the core (indicated with arrow, H). Additional ultrastructural features characterized by multiple areas of sarcomere disruption (J-L) of variable size, with fragmentation of Z-lines and loss of M-bands.

Please cite this article as: S.J. Beecroft, M. Olive and L.G. Quereda et al., Cylindrical spirals in two families: Clinical and genetic investigations, Neuromuscular Disorders, https://doi.org/10.1016/j.nmd.2019.12.006

showed a second, smaller PCR product that was absent from the control (Fig. 2A). Sanger sequencing of the PCR product showed the creation of a cryptic GT splice donor at c.15925, causing skipping of exon 54 from c.15925-16,054 (Fig. 2B). The altered splicing created an early stop codon p.Ser5310Glu*fs**34, likely resulting in nonsense-mediated decay. The fainter band for the smaller product suggested less abundance of this truncated transcript. See Fig. 2C for a schematic representation of the splicing defect.

4. Discussion

The rarity of ultrastructural myopathies has limited investigation into their genetic and mechanistic origins. We present two families with *EBF3* and *TTN* variants harbouring cylindrical spirals in their muscle biopsy. Inclusions within muscle from both families were detected by H&E, modified Gomori trichrome, NADH staining and electron microscopy consistent with the histochemical and ultrastructural signatures identified by other authors [3,6,12].

EBF3 is a highly conserved transcription factor from the Collier/Olf/EBF (COE). Heterozygous mutations were first associated with human disease in 2017, causing a neurodevelopmental phenotype [19,29–32]. An additional report suggested the effect was due to haploinsufficiency as opposed to a dominant-negative effect [33]. Family AUS1 initially was referred for research with the diagnosis of 'cylindrical spiral myopathy' based on their muscle biopsy results. Upon reconsideration by the clinician, the features of facial weakness [19,29,30,33], delayed walking [19,29,30], prominent chin [29,33], speech delay [29–31,33], and hypotonia [19,29,30] in this family were found to be consistent with the *EBF3* phenotype. However, the scoliosis in family AUS1 was much more severe than previously described, requiring surgery in both affected individuals. Further review of the clinical history allowed us to link several features seen in AUS1 II:2 with those seen in other *EBF3* patients, including esotropia [19,31], genitourinary problems [19,29–31], pectus excavatum [19,31], behavioural difficulties and attentional challenges [19,33], difficulty feeding [19,29], recurrent otitis media [33] (also seen in his unaffected brother), difficulty with swallowing some foods [29] and perservative social behaviours [30]. His mother's *pes planus* [19,33] and shortened large toe [19] were also previously reported with the *EBF3* phenotype. The cramps seen in family AUS1 have not been described previously in patients with *EBF3* mutations. No other reported patient has had a muscle biopsy, so it is uncertain if cylindrical spirals are a common feature of *EBF3*-related disease. The cylindrical spirals may be a non-specific feature in this family. Further cases will assist in clarifying the association of cylindrical spirals with *EBF3* disease. We were unable to obtain further muscle or fibroblasts to perform further investigations for family AUS1. It seems likely that there may be a group of patients with a muscle and brain phenotype caused by *EBF3* pathogenic variants. Further characterisation of the *EBF3* phenotypic spectrum is required.

Cylindrical spirals have been noted in two families with ataxia [2,7]. The first report was a 53-year-old man with a familial form of progressive ataxia, diagnosed as hereditary spinocerebellar degeneration [2]. The second family was clinically diagnosed with Behr's syndrome (OMIM #210000) [7]. Attempts to obtain archived genetic material from the 53-year-old patient were unsuccessful. Although *EBF3* is primarily recognised for its effect on neural development, a 2014 report showed that murine *Ebf3* is involved in the regulation of muscle cell-specific transcription [34]. *Ebf3* synergises with MyoD to induce expression of *Atp2a1* in the murine diaphragm. All four Ebf factors synergised with MyoD to induce *Atp2a1* expression in muscle cells [34]. *ATP2A1* encodes SERCA1, one of six sarcoplasmic/endoplasmic reticulum Ca^{2+} ATPases [35]. These proteins catalyse the transport of cytoplasmic Ca^{2+} to the SR/ER lumen [35]. Mutations in *ATP2A1* are associated with Brody myopathy (OMIM #601003), which is characterised by muscle stiffness, impaired muscle relaxation and cramps due to reduced SERCA1 activity [36]. The reduction in SERCA1 activity delays the clearance of intracellular Ca^{2+} after muscle contraction, resulting in extended periods of high sarcoplasmic Ca^{2+} [36,37]. Excessive intracellular Ca^{2+} is a known trigger for tubular aggregate formation [14,38] (seen in family AUS1, in addition to cylindrical spirals). Tubular aggregates appear to act as a Ca^{2+} sink, mitigating the effects of intracellular hypercalcemia [39]. Given the overlap between cylindrical spirals and tubular aggregates, cylindrical spirals may also be involved in regulating Ca^{2+} homeostasis. Previous studies showed that addition of $Ca^{2+}$to sonicated preparations of phosphatidylserine in aqueous NaCl buffer produces spiral-shaped lipid cylinders that develop into flattened sheets, which then form coiled, elongated multilamellar cylinders [5].

We postulate that haploinsufficiency of *EBF3* may cause a downstream reduction in SERCA1 activity, causing sarcoplasmic hypercalcaemia and tubular aggregate/cylindrical spiral formation in some patients. The muscle cramps upon exercise experienced by the affected individuals in Family AUS1 support this possibility. However, without further patient tissue from this family, or muscle biopsy from another *EBF3* patient to confirm this finding, this remains a hypothesis.

The clinical presentation of proband SPA1 fits well with congenital titinopathy [40]. The combination of two truncating variants was deemed sufficient to attribute *TTN* as the genetic cause of disease in this patient under ACMG guidelines [20]. Cylindrical spirals have not been reported as a pathological feature in the muscle of patients with titinopathy, to the best of our knowledge. Given the high volume of published titinopathy patients, the cylindrical spirals in our patient may represent a particularly rare finding in recessive titinopathy. Additional pathological features including high numbers of internal nuclei, core-like lesions on oxidative stains, and the ultrastructural features showing sarcomeric disruption have been previously reported in titinopathy patients [41,42]. Although titin and Ca^{2+} have been shown to interact [43,44],

Please cite this article as: S.J. Beecroft, M. Olive and L.G. Quereda et al., Cylindrical spirals in two families: Clinical and genetic investigations, Neuromuscular Disorders, https://doi.org/10.1016/j.nmd.2019.12.006

there does not appear to be a distinct mechanism linking titin and cylindrical spirals via Ca^{2+} handling. Another possibility is that given the complexity of *TTN* alternative splicing [45], only particular pathogenic variants (or combinations thereof) may be likely to cause cylindrical spirals. Additionally, we cannot exclude that the cylindrical spirals are a non-specific finding in this case. We suspect that cylindrical spirals will come to be associated with other genetic variants.

Acknowledgments

We extend our sincere thanks to the families involved in this study. SJB is funded by The Fred Liuzzi Foundation (TFLF) (Melbourne, Australia). NGL (APP1117510) and GR (APP1122952) are supported by the Australian National Health and Medical Research Council (NHMRC). GR is also supported by a Western Australian Department of Health Future Health's WA Merit Award. This work is funded by TFLF and NHMRC (APP1080587). M.O. is supported by a grant from ISCIII PI14/00738, and FEDER funds "a way to achieve Europe''. P. G. is supported by a grant from ISCIII PI 15/01898, and FEDER funds "a way to achieve Europe''. The funding agencies were not involved in the design, completion, or writing of this study. The authors would like to thank the Genome Aggregation Database (gnomAD) and the groups that provided exome and genome variant data to this resource. A full list of contributing groups can be found at https://gnomad.broadinstitute.org/about.

References

[1] Xu JW, Liu FC, Li W, Zhao YY, Zhao DD, Luo YB, et al. Cylindrical spirals in skeletal muscles originate from the longitudinal sarcoplasmic reticulum. J Neuropathol Exp Neurol 2016;75:148–55. doi:10.1093/jnen/nlv013.

[2] Carpenter S, Karpati G, Robitaille Y, Melmed C. Cylindrical spirals in human skeletal muscle. Muscle Nerve 1979;2:282–7. doi:10.1002/mus.880020407.

[3] Bove KE, Iannaccone ST, Hilton PK, Samaha F. Cylindrical spirals in a familial neuromuscular disorder. Ann Neurol 1980;7:550–6. doi:10.1002/ana.410070608.

[4] Mcdougall J, Wiles CM, Edwards RHT. Spiral membrane cylinders in the skeletal muscle of a patient with melorheostosis. Neuropathol Appl Neurobiol 1980;6:69–74. doi:10.1111/j.1365-2990.1980.tb00205.x.

[5] Gibbels E, Henke U, Schädlich H-J, Haupt WF, Fiehn W. Cylindrical spirals in skeletal muscle: a further observation with clinical, morphological, and biochemical analysis. Muscle Nerve 1983;6:646–55. doi:10.1002/mus.880060905.

[6] Danon MJ, Carpenter S, Harati Y. Muscle pain associated with tubular aggregates and structures resembling cylindrical spirals. Muscle Nerve 1989;12:265–72.

[7] Thomas PK, Workman JM, Thage O. Behr's syndrome. J Neurol Sci 1984;64:137–48. doi:10.1016/0022-510X(84)90032-7.

[8] Sadalage G, Jacob S. Tubular aggregates and cylindrical spirals in autoimmune limb-girdle myasthenia. J Neurol Neurosurg Psychiatry 2016;87:e1 88-e1. doi:10.1136/jnnp-2016-315106.178.

[9] Malfatti E, Chaves M, Bellance R, Viou MT, Sarrazin E, Fardeau M, et al. Cylindrical spirals associated with severe congenital muscle weakness and epileptic encephalopathy. Muscle Nerve 2015;52:895–9. doi:10.1002/mus.24699.

[10] Taratuto AL, Matteucci M, Barreiro C, Saccolitti M, Sevlever G. Autosomal dominant neuromuscular disease with cylindrical spirals. Neuromusc Disord 1991;1:433–41. doi:10.1016/0960-8966(91)90006-E.

[11] Yamamoto H, Sahashi K, Mizuno Y, Ibi T, Sobue G. [A case of a mitochondrial myopathy with cylindrical spirals (author's transl)]. Rinsho Shinkeigaku 1982;22:244–50.

[12] Brady S, Healy EG, Gang Q, Parton M, Quinlivan R, Jacob S, et al. Tubular aggregates and cylindrical spirals have distinct immunohistochemical signatures. J Neuropathol Exp Neurol 2016;75:1171–8. doi:10.1093/jnen/nlw096.

[13] Chevessier F, Bauché-Godard S, Leroy J-P, Koenig J, Paturneau-Jouas M, Eymard B, et al. The origin of tubular aggregates in human myopathies. J Pathol 2005;207:313–23. doi:10.1002/path.1832.

[14] Böhm J, Laporte J. Gain-of-function mutations in STIM1 and ORAI1 causing tubular aggregate myopathy and stormorken syndrome. Cell Calcium 2018;76:1–9. doi:10.1016/j.ceca.2018.07.008.

[15] Beecroft SJ, McLean CA, Delatycki MB, Koshy K, Yiu E, Haliloglu G, et al. Expanding the phenotypic spectrum associated with mutations of DYNC1H1. Neuromuscul Disord 2017;27:607–15. doi:10.1016/j.nmd.2017.04.011.

[16] McLaren W, Gil L, Hunt SE, Riat HS, Ritchie GRS, Thormann A, et al. The ensembl variant effect predictor. Genome Biol 2016;17:122. doi:10.1186/s13059-016-0974-4.

[17] Paila U, Chapman BA, Kirchner R, Quinlan AR. GEMINI: integrative exploration of genetic variation and genome annotations. PLoS Comput Biol 2013;9:e1003153. doi:10.1371/journal.pcbi.1003153.

[18] Sanger F, Nicklen S, Coulson AR. DNA sequencing with chain-terminating inhibitors. Proc Natl Acad Sci U S A 1977;74:5463–7.

[19] Sleven H, Welsh SJ, Yu J, Churchill MEA, Wright CF, Henderson A, et al. De novo mutations in EBF3 cause a neurodevelopmental syndrome. Am J Hum Genet 2017;100:138–50. doi:10.1016/j.ajhg.2016.11.020.

[20] Richards S, Aziz N, Bale S, Bick D, Das S, Gastier-Foster J, et al. Standards and guidelines for the interpretation of sequence variants: a joint consensus recommendation of the american college of medical genetics and genomics and the association for molecular pathology. Genet Med 2015;17:405–24. doi:10.1038/gim.2015.30.

[21] Lek M, Karczewski KJ, Samocha KE, Banks E, Fennell T, O AH, et al. Analysis of protein-coding genetic variation in 60,706 humans. Nature 2016;536:285–92.

[22] Cartegni L, Wang J, Zhu Z, Zhang MQ, Krainer AR. ESEfinder: a web resource to identify exonic splicing enhancers. Nucl Acids Res 2003;31:3568–71. doi:10.1093/nar/gkg616.

[23] Smith PJ, Zhang C, Wang J, Chew SL, Zhang MQ, Krainer AR. An increased specificity score matrix for the prediction of SF2/ASF-specific exonic splicing enhancers. Hum Mol Genet 2006;15:2490–508. doi:10.1093/hmg/ddl171.

[24] Raponi M, Kralovicova J, Copson E, Divina P, Eccles D, Johnson P, et al. Prediction of single-nucleotide substitutions that result in exon skipping: identification of a splicing silencer in BRCA1 exon 6. Hum Mutat 2011;32:436–44. doi:10.1002/humu.21458.

[25] Pertea M, Lin X, Salzberg SL. GeneSplicer: a new computational method for splice site prediction. Nucl Acids Res 2001;29:1185–90. doi:10.1093/nar/29.5.1185.

[26] Desmet FO, Hamroun D, Lalande M, Collod-Bëroud G, Claustres M, Béroud C. Human splicing finder: an online bioinformatics tool to predict splicing signals. Nucl Acids Res 2009:37. doi:10.1093/nar/gkp215.

[27] Yeo G, Burge CB. Maximum entropy modeling of short sequence motifs with applications to rna splicing signals. J Comput Biol 2004;11:377–94. doi:10.1089/1066527041410418.

[28] Fairbrother WG, Yeh RF, Sharp PA, Burge CB. Predictive identification of exonic splicing enhancers in human genes. Science 2002;297(80–):1007–13. doi:10.1126/science.1073774.

[29] Harms FL, Girisha KM, Hardigan AA, Kortum F, Shukla A, Alawi M, et al. Mutations in EBF3 disturb transcriptional profiles and underlie a novel syndrome of intellectual disability, ataxia and facial dysmorphism. Am J Hum Genet 2016;100:117–27. doi:10.1101/067454.

[30] Chao H-TT, Davids M, Burke E, Pappas JG, Rosenfeld JA, McCarty AJ, et al. A syndromic neurodevelopmental disorder caused by de novo variants in EBF3. Am J Hum Genet 2017;100:128–37. doi:10.1016/j.ajhg.2016.11.018.

[31] Blackburn PR, Barnett SS, Zimmermann MT, Cousin MA, Kaiwar C, Pinto e Vairo F, et al. Novel de novo variant in EBF3 is likely to impact DNA binding in a patient with a neurodevelopmental disorder and expanded phenotypes: patient report, in silico functional assessment, and review of published cases. Mol Case Stud 2017;3:a001743. doi:10.1101/mcs.a001743.

[32] Tanaka AJ, Cho MT, Willaert R, Retterer K, Zarate YA, Bosanko K, et al. De novo variants in EBF3 are associated with hypotonia, developmental delay, intellectual disability, and autism. Mol Case Stud 2017;3:a002097. doi:10.1101/mcs.a002097.

[33] Lopes F, Soares G, Gonçalves-Rocha M, Pinto-Basto J, Maciel P. Whole gene deletion of EBF3 supporting haploinsufficiency of this gene as a mechanism of neurodevelopmental disease. Front Genet 2017:8. doi:10.3389/fgene.2017.00143.

[34] Jin S, Kim J, Willert T, Klein-Rodewald T, Garcia-Dominguez M, Mosqueira M, et al. Ebf factors and myod cooperate to regulate muscle relaxation via atp2a1. Nat Commun 2014;5:3793. doi:10.1038/ncomms4793.

[35] Pan Y, Zvaritch E, Tupling AR, Rice WJ, De Leon S, Rudnicki M, et al. Targeted disruption of the ATP2A1 gene encoding the sarco(endo)plasmic reticulum Ca2+ ATPase isoform 1 (SERCA1) impairs diaphragm function and is lethal in neonatal mice. J Biol Chem 2003;278:13367–75. doi:10.1074/jbc.M213228200.

[36] Voermans NC, Laan AE, Oosterhof A, van Kuppevelt TH, Drost G, Lammens M, et al. Brody syndrome: a clinically heterogeneous entity distinct from brody disease. Neuromuscul Disord 2012;22:944–54. doi:10.1016/j.nmd.2012.03.012.

[37] De Ruiter CJ, Wevers RA, Van Engelen BG, Verdijk PW, De Haan A. Muscle function in a patient with brody's disease. Muscle Nerve 1999;22:704–11.

[38] Böhm J, Chevessier FF, De Paula AMAM, Koch C, Attarian S, Feger C, et al. Constitutive activation of the calcium sensor STIM1 causes tubular-aggregate myopathy. Am J Hum Genet 2013;92:271–8. doi:10.1016/j.ajhg.2012.12.007.

[39] Salviati G, Pierobon-Bormioli S, Betto R, Damiani E, Angelini C, Ringel SP, et al. Tubular aggregates: sarcoplasmic reticulum origin, calcium storage ability, and functional implications. Muscle Nerve 1985;8:299–306. doi:10.1002/mus.880080406.

[40] Savarese M, Sarparanta J, Vihola A, Udd B, Hackman P. Increasing role of titin mutations in neuromuscular disorders. J Neuromuscul Dis 2016;3:293–308. doi:10.3233/JND-160158.

[41] Carmignac V, Salih MAM, Quijano-Roy S, Marchand S, Al Rayess MM, Mukhtar MM, et al. C-terminal titin deletions cause a novel early-onset myopathy with fatal cardiomyopathy. Ann Neurol 2007;61:340–51. doi:10.1002/ana.21089.

[42] Ávila-Polo R, Malfatti E, Lornage X, Cheraud C, Nelson I, Nectoux J, et al. Loss of sarcomeric scaffolding as a common baseline histopathologic lesion in titin-related myopathies. J Neuropathol Exp Neurol 2018;77:1101–14. doi:10.1093/jnen/nly095.

[43] Ottenheijm CAC, Hidalgo C, Rost K, Gotthardt M, Granzier H. Altered contractility of skeletal muscle in mice deficient in titin's M-Band region. J Mol Biol 2009;393:10–26. doi:10.1016/j.jmb.2009.08.009.

[44] Peng J, Raddatz K, Molkentin JD, Wu Y, Labeit S, Granzier H, et al. Cardiac hypertrophy and reduced contractility in hearts deficient in the Titin kinase region. Circulation 2007;115:743–51. doi:10.1161/CIRCULATIONAHA.106.645499.

[45] Savarese M, Jonson PH, Huovinen S, Paulin L, Auvinen P, Udd B, et al. The complexity of titin splicing pattern in human adult skeletal muscles. Skelet Muscle 2018;8:11. doi:10.1186/s13395-018-0156-z.

Please cite this article as: S.J. Beecroft, M. Olive and L.G. Quereda et al., Cylindrical spirals in two families: Clinical and genetic investigations, Neuromuscular Disorders, https://doi.org/10.1016/j.nmd.2019.12.006